

Characterization of deformation behaviour and fracture mode of recycled aluminium alloys (AA6061) subjected to high-velocity impact

C. S. Ho¹ and M. K. Mohd Nor^{1*}

¹Crashworthiness and Collisions Research Group (COLOURED), Mechanical Failure Prevention and Reliability Research Center (MPROVE), Faculty Mechanical and Manufacturing Engineering, Universiti Tun Hussein Onn Malaysia, Parit Raja, 86400 Batu Pahat, Johor, Malaysia

ABSTRACT – Recycling aluminium alloys have been shown to provide great environmental and economic benefits. The global demands placed upon recycled aluminium and its product has further increased the need for better understanding and prediction of the deformation behaviour of such materials subjected to various dynamic loading conditions. It is also a topic of high interest for both the designer and the user of metal structures, specifically in the automotive industry. Even though numerous efforts have been made to improve recycling processes of aluminium alloys, very little attention is given on the fracture behaviour related damage and anisotropy during impact. In this study, therefore, the anisotropic-damage behaviour of the recycled aluminium alloys (AA6061) is examined via Taylor Cylinder Impact test. A gas gun was used to fire the projectiles towards a target at impact velocity ranging from 170m/s to 370 m/s. The deformation behaviour, including the fracture modes, digitized footprint and side profile of the deformed specimens, are observed and analysed. Scanning Electron Microscope (SEM) is further used to observe the damage behaviour, including microstructural changes of the impact surface. The damage progression is also analysed by observing the microstructural behaviour of location 0.5 cm from the impact area. General speaking, there are three different types of ductile fracture modes (mushrooming, tensile splitting and petalling) can be observed in this study within the impact velocity range of 170m/s to 370m/s. The critical impact velocity is defined at 212 m/s. The digitized footprint analysis exhibited a non-symmetrical (ellipse-shaped) footprint where the footprints showed plastic anisotropic behaviour and localized plastic strain in such recycled material. The damage evolution of the material is increasing with the increase in impact velocity.

ARTICLE HISTORY

Revised: 08th Apr 2020

Accepted: 01st May 2020

KEYWORDS

*Recycled aluminium alloys,
Taylor cylinder impact test;
anisotropic-damage;
fracture modes;
damage progression*

INTRODUCTION

Aluminium is one of the most famous metals applied in various industry sectors and applications, for such building, machinery, packaging, automobile industry, and aerospace application. It is widely employed due to the excellent strength and high strength to density ratio properties, which able to enhance the crashworthiness and reduce the weight of the component [1, 2]. For a pure aluminium combination, it has delicate and low-quality properties. So, with a specific end goal to improve the quality, others components, for example, Magnesium (Mg), Silicon (Si), Copper (Cu), Zinc (Zn), Lithium (Li) and Manganese (Mn) are included and mixed into an aluminium synthesis [3].

Furthermore, the demand for aluminium alloy has been increasing yearly since the beginning of the industrial revolution in 1760. It is due to the excellent mechanical properties of the aluminium alloys such as high strength, low density, easy for machining, and corrosion resistance [4]. However, the production processes in producing aluminium are hugely energy-intensive and may lead to pollution as aluminium is produced initially from bauxite. Thus, to reduce pollution and save energy, aluminium recycling is encouraged, which capable of saving about 95% of the energy [5], [6].

Nowadays, aluminium recycling has become a well-known topic and many aluminium solid-state recycling methods that had been studied and introduced by researchers, for instance, direct recycling via cold compression [7, 8], powder metallurgy [5, 9–12], hot extrusion [13–16], and hot press forging [3, 17–19]. In the present study, hot press forging of the direct conversion recycling process is adopted to form the specimen [20]. Although the optimum setting for the recycling process had been conducted and defined in previous studies, the numerous concerns related to damage behaviour of such recycled material are still to be answered. Most of the engineering materials show orthotropic behaviour when undergoing elastoplastic deformation [21, 22]. The prediction of such recycled material undergoing finite strain deformation including damage evolution is still an open and exciting area of study. In the real applications, the probabilities of a material to collide with other objects in different impact velocities could occur, especially in automobile applications. The impact might lead to damage and catastrophic failure of the materials [23].

Damage can be described as a set of permanent microstructural changes altering thermo-mechanical properties. Also, it acquires an arrangement of irreversible physical micro-cracking forms due to the utilization of thermo-mechanical loading [24, 25]. In aluminium composites, damage can be identified with advancing microstructural highlights. The failure procedure in flexible materials is related to the nearby failure of second stage particles, incorporations,

intermetallic particles, and precipitates. For instance, [26] demonstrated that the splitting of particles in A357 aluminium composite happens amid plastic deformation.

Balasundaram et al. [27] have reported that damage in aluminium compounds is created by breaking of intermetallic particles, development of voids at broke particles and void mixture. The investigation verified that the heading of breaks under pressure loading was opposite to the heap course. Along these lines, the approach for distinguishing damage of aluminium composite is essential for evaluating parts lifespan in the car, aviation, hardware, and other metal-based industry. It should be noted that the harm is numerously related to the primary reaction of the material microstructure subjected to various loading conditions.

Besides, the damage progression is also significant in a better understanding of such recycled material. When a material hit a target plate, the particle on the impact surface is brought to the rest relative to the target face immediately, and shock is formed. The shock wave formed leads to each succeeding layer of the particle to rest, and causing damage progression. The field of impact progression covers various circumstances is vital to engineers from different distinctive areas [28, 29]. For instance, production engineers are keen regarding the matter in regards of its application to fast blanking and opening flanging forms while vehicle makers utilize their comprehension of the reaction of structures to impact loading to enhance the execution and security of their items.

Notwithstanding, high-velocity impact mainly centred on primary metals explored by numerous analyst. Conversely, the recycling metals experience a high-velocity impact to a great extent unexplored. Most materials demonstrated considerable changes in the mechanical reaction under expanded rates of stressing [30, 31]. In the field of crash and impact modelling, Taylor cylinder impact test can be regarded as one of the best approaches to investigate damage progression under the high-velocity impact. The test is named after G. I. Taylor, who developed the test to screen materials in ballistic applications during world war II [32]. This test entails firing a solid cylinder rod of material under consideration, typically 7.5 to 12.5 mm in diameter by 25 to 40 mm in length, at high velocity against a massive and plastically rigid target.

Taylor cylinder impact testing has previously been utilized to probe both the deformation responses of metals and alloys in the presence of large gradients of stress, strain and strain-rate and as a means to validate constitutive models [33]. This axis-symmetric integrated test provides a readily conducted experimental method to examine the large-strain high-strain rate mechanical behaviour of materials, at the same time evaluating the accuracy of appropriate “physics” incorporation in constitutive models. It is simple, inexpensive, and exhibits large strains, high-strain rates at elevated temperatures. Further, this test is also used to estimate or to validate high-strain rate material constants under dynamic loading conditions.

Besides, Rakvåg, Børvik and Hopperstad [34] studied the behaviour of steel and its fracture mode via the Taylor impact test. The materials with different hardness are tested at different impact velocity, and the deformation and its fracture mode are observed. Metallurgical analysis of fracture surface using a Scanning Electron Microscope (SEM) also had been conducted. Generally speaking, there are five different deformations and fracture modes were revealed, as shown in Figure 1. The deformation and fracture mode is deformed with the changes in impact velocity [34, 35].

In this study, the Taylor cylinder impact test is adopted to examine damage evolution, and damage progression in deformed specimens due to high shock pressures and plastic strains can be produced during the test. In this setting, the deformable flat-nosed cylinders are fired against a fixed quasi-rigid wall that allows for material behaviour estimation at high-strain rates. The post-geometry of the cylindrical specimen is examined in terms of final length, major side profile and the deformed footprint in addition to post-mortem microstructural analysis.

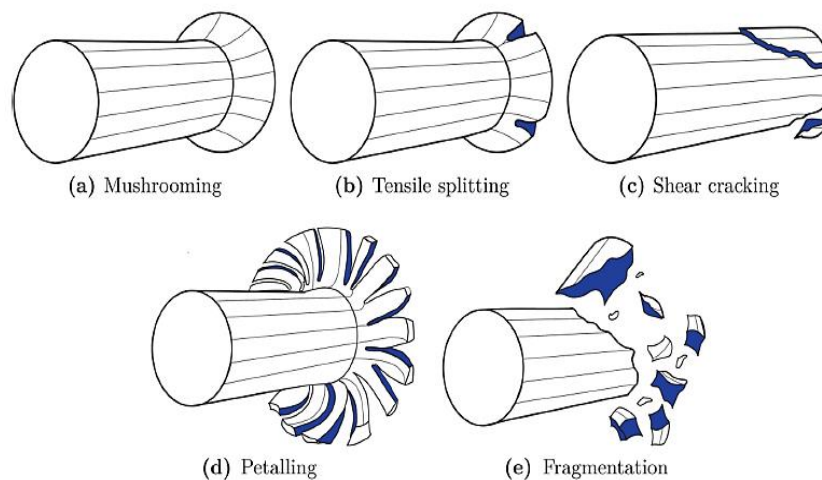


Figure 1. Impact deformation and fracture mode [35]

EXPERIMENTAL PROCEDURE

It is crucial to study the damage progression and its anisotropic behaviour, including the fracture mode of a material undergoing high-velocity impact, to analyze the potential of the material in the advanced application. There are many techniques used to predict the deformation process of structure and components at various strain rates. In the present study, the Taylor impact test is used due to its economy, simplicity and the opportunity to yield valuable data at high strain rate [36]. The following discussed further the experimental procedure adopted in this study.

Specimen Preparation

Figure 2 illustrates the procedure of specimen preparation. First of all, the chips are produced with an average rectangular shape chips size of 5.2 mm length x 1.097 mm width x 0.091 mm thickness using MAZAK vertical centre Nexus 410A-II- CNC machine with the machining setting as shown in Table 1. Next, Acetone solution is used to clean the chips by using the ultrasonic bath and dried in a 60°C thermal oven for about 30 minutes. Subsequently, hot press forging recycling technique with the optimum forming process parameter referring to the previous study by [3, 19] is adopted to form the recycled specimen. Specifically, the process is performed at a constant temperature and pressure of 530°C and 47 MPa (35.6 tons), respectively, with 2 hours holding time. Then, the hot-forged specimen is quenched at 100°C/s quench rate and instantaneously artificial ageing by putting the specimen in a 175°C thermal oven for 120 minutes. The final specimen is then denoted as T5-temper. Lastly, the electrical wire cutting machine is used to form the specimen into a cylindrical shape with length and diameter of 15mm and 8.45mm, respectively, as shown in Figure 3.

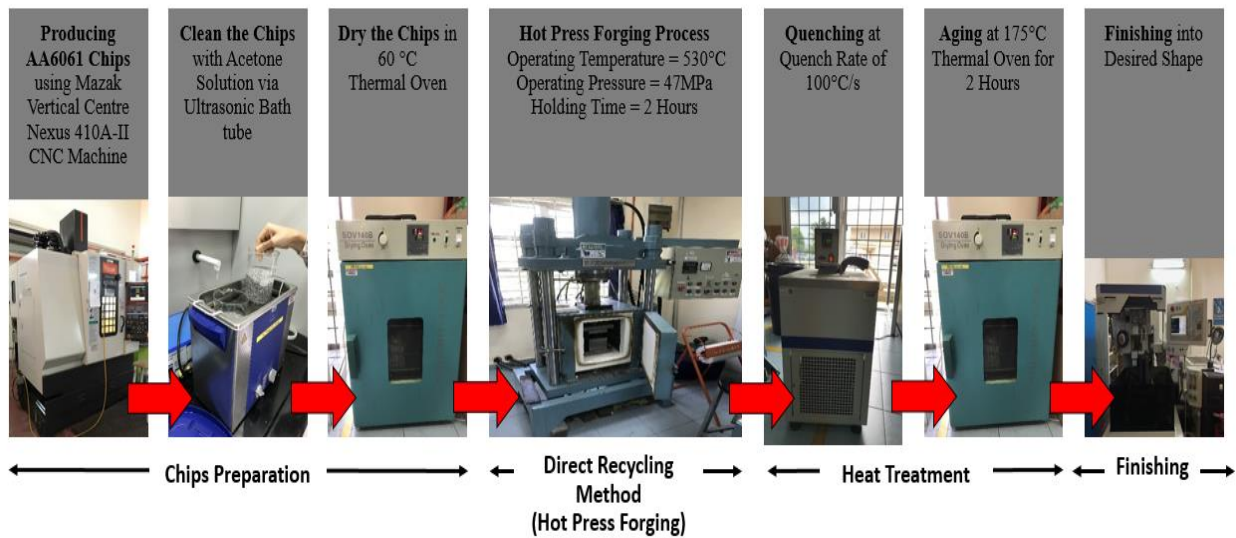


Figure 2. Flow of specimen preparation

Table 1. Chips milling parameters

| Parameter | Value | Geometry of Chips |
|------------------|---------------|--|
| Cutting Speed, v | 377 m/min |  |
| Diameter tool | 10 mm | |
| Feed, f | 0.05 mm/tooth | |
| Depth of Cut | 1 mm | |

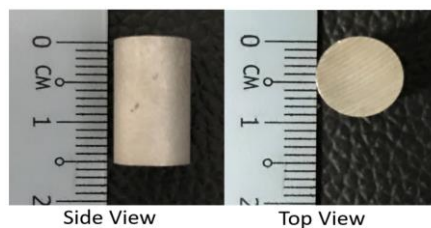


Figure 3. Cylindrical shaped specimen

Experimental Setup

The Taylor cylinder impact test is conducted in this work by launching a cylindrical specimen a smooth bored gun barrel to the rigid massive hardened stainless steel target. To ensure the effect of friction is minimized, the target surface is polished to a mirror-like finished [37]. Figure 4 shows the setup of the impact gas gun machine used in this research. The pressure is used as a force to launch the bullet toward the target. The high-speed camera is utilized to capture the movement and deformation of the bullet towards the target and measure the impact velocity. The high-speed camera having resolution times of less than one-tenth microsecond, in which the deformation is captured in the inter-frame of 4 microseconds, which equivalent to the 250,000 frames per second. Table 2 shows the experimental design used in this study with initial length (L_0) and diameter (D_0) of 1.5mm and 8.45mm, respectively.. The specimens are tested in 10 different impact velocity ranging from 170 m/s to 370 m/s. The range of the impact velocity is selected based on the capability of the gas-gun machine, where the maximum pressure that can be set able to produce maximum impact velocity to about 370m/s. The minimum impact velocity is chosen based on preliminary study in [38]. The impact surface and the sectional cut area (about 5 mm away from the impact surface) of the specimens, as shown in Figure 5, are observed under SEM machine to study the microstructure of the material related to damage and its propagation.

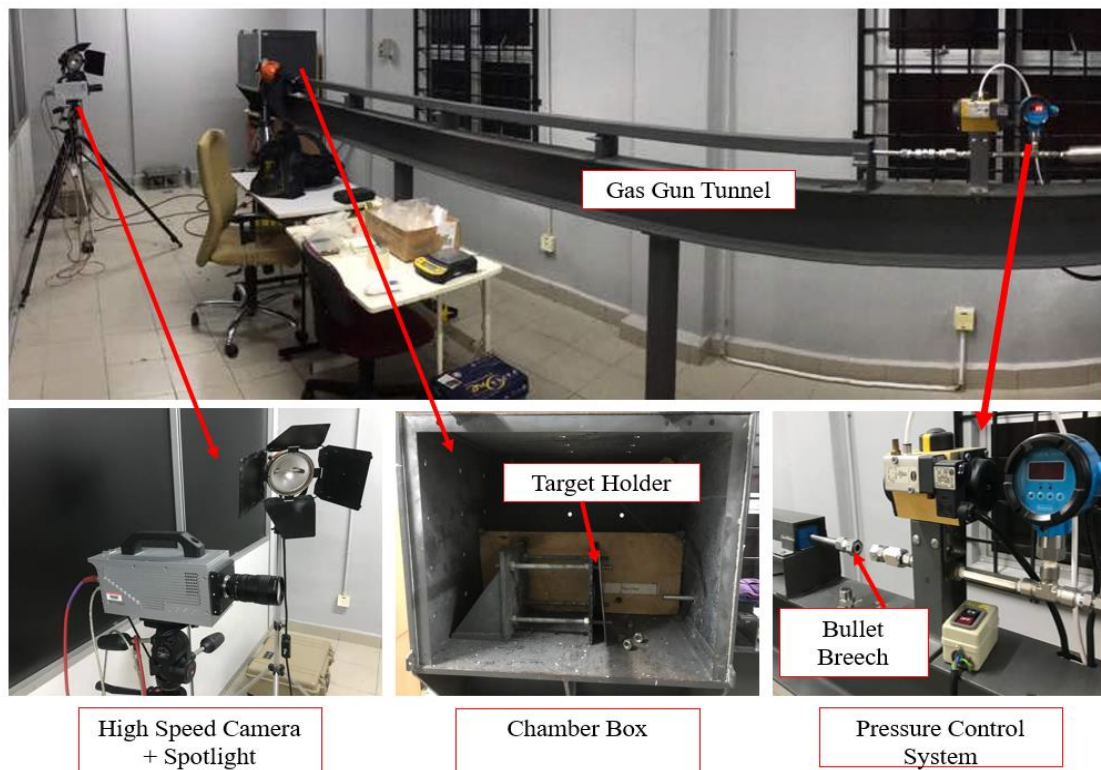


Figure 4. Impact gas gun machine

Table 2. Test matrix for Taylor cylinder impact test

| Test No. | Impact Velocity, V (m/s) |
|----------|----------------------------|
| 1 | 170 – 189 |
| 2 | 190 – 209 |
| 3 | 210 – 229 |
| 4 | 230 – 249 |
| 5 | 250 – 269 |
| 6 | 270 – 289 |
| 7 | 290 – 309 |
| 8 | 310 – 329 |
| 9 | 330 – 349 |
| 10 | 350 – 370 |

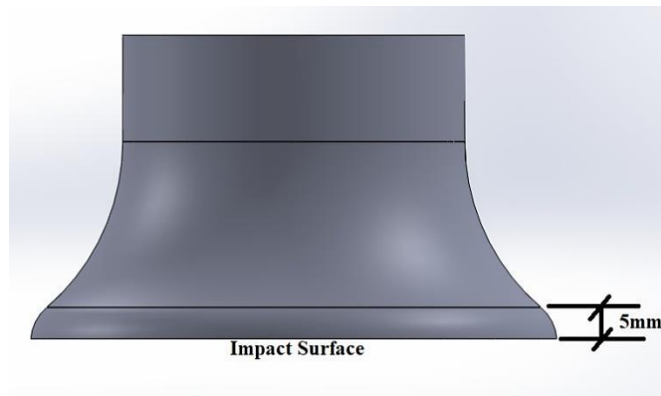


Figure 5. Schematic diagram of sectional cut area for SEM

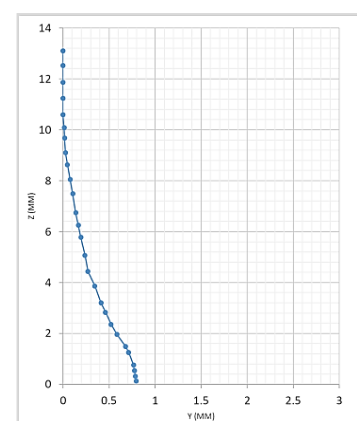
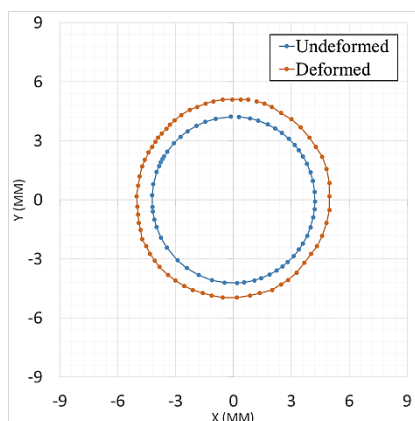
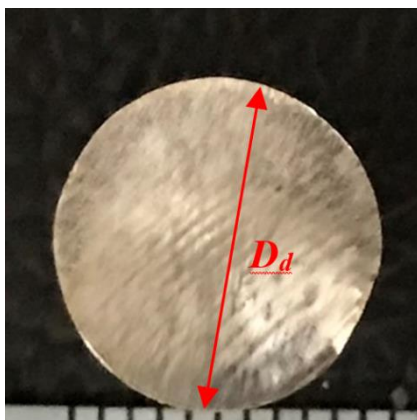
RESULTS AND DISCUSSIONS

This section summarises the result of the Taylor impact test. The damage behaviour of the recycled material at different impact velocity can be observed by measuring the deformed length, deformed diameter, and observing the fracture mode. After the testing, the data and geometric profile of the deformed specimens are generated using a 3D scanner. Besides, the microstructure of the impact specimen is investigated under a scanning electron microscope (SEM).

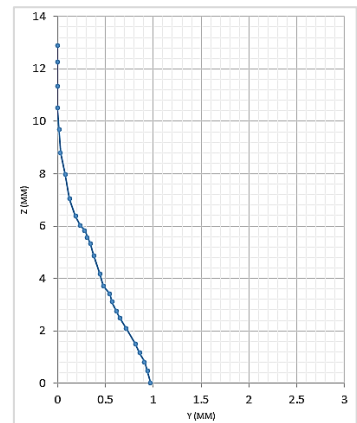
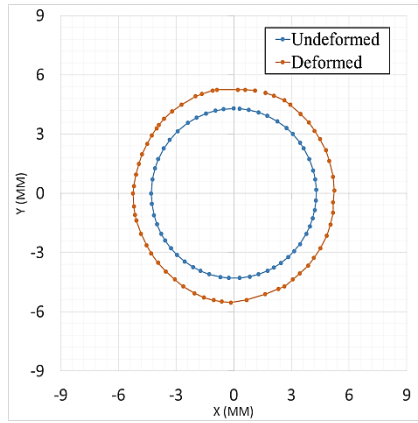
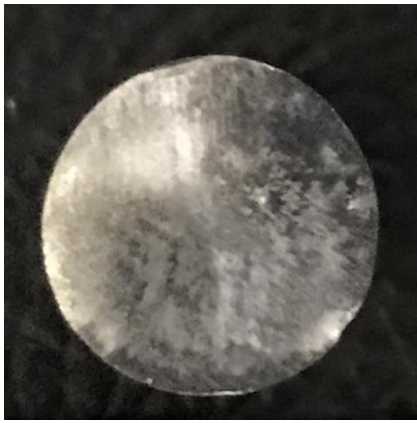
Fracture Mode and 3D Scanning Analysis

In the Taylor cylinder impact test, the differences in fracture mode and deformation behaviour are observed on the specimen tested at different impact velocities. The maximum impact velocity that can be achieved by the gas gun machine for such recycled material with length and diameter of 15mm and 8.45mm, respectively, was about 367 m/s. Also, the deformed specimens were scan with a 3D scanner to obtain the digitized data of geometric profile.

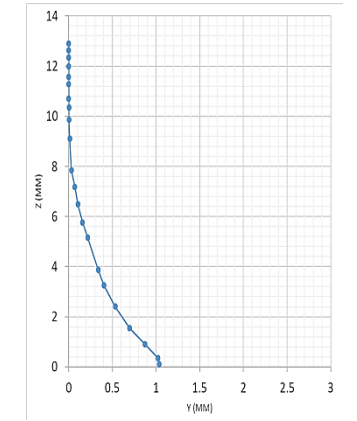
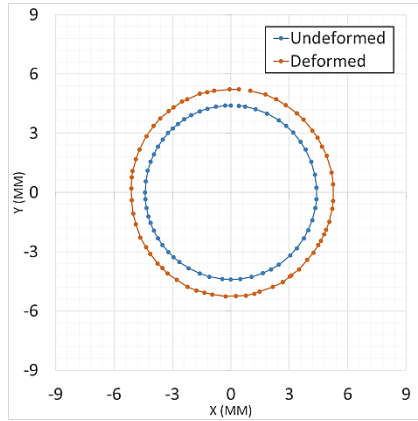
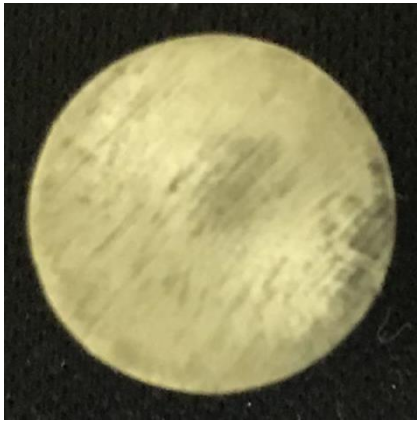
Figure 6 depicts the deformed footprint and its 3D-scan digitized footprint and major side profile after impact at various velocities. For the footprint digitized data, orange lines represent the impact surface, and blue lines denoted the initial dimension of the specimen. It can be observed that the dimension of the impact surface is getting more significant as the impact velocity increases. Cracks are found to initiate at the edge of the footprint from impact velocity of 230.58m/s, and petalling edge is formed from the impact velocity 328.81 m/s. Generally speaking, the recycled AA6061 exhibited strong plastic anisotropic behaviour undergoing finite strain deformation. The deformed footprint distorted evidently in various directions, and the footprint shows an ellipse (non-symmetric) shaped. In the contrarily, from the digitized side profile data, the length of the specimen is observed decreases about 1 to 4 mm from the initial length within the velocity range of 179 – 367 m/s. The length of the deformed specimen is associated with the amount of deformation. The deformed specimen at lower impact velocities ($V= 179 - 257$ m/s) exhibited little deformation; while, at higher impact velocities ($V= 287 - 367$ m/s), the specimen shown more localized deformations.



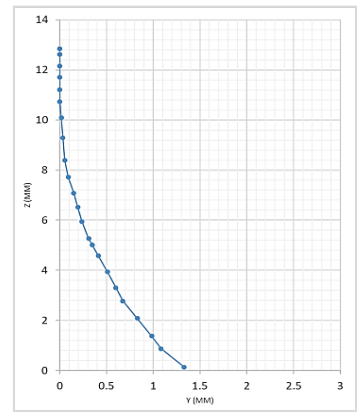
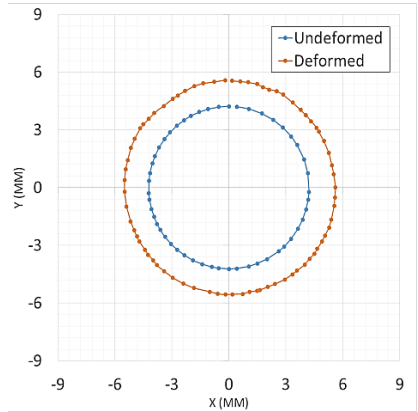
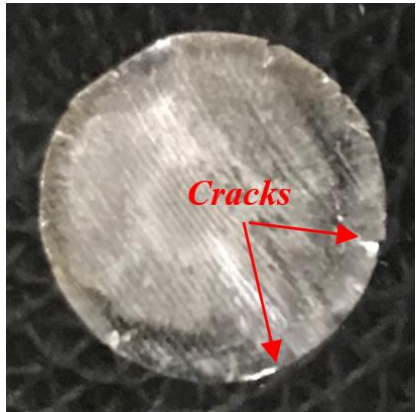
(a) $V= 179.01$ m/s



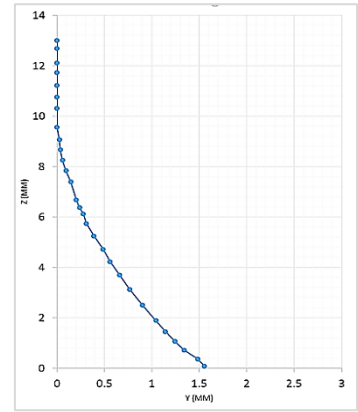
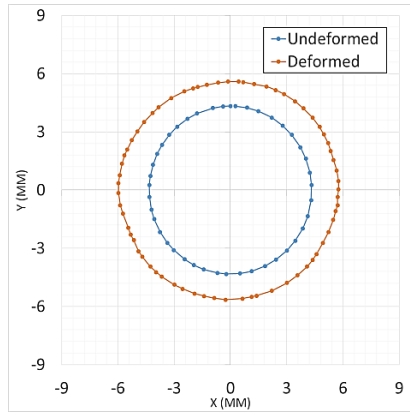
(b) $V=195.28$ m/s



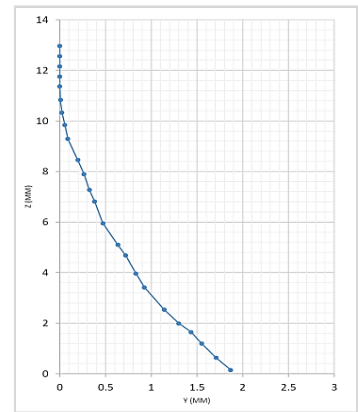
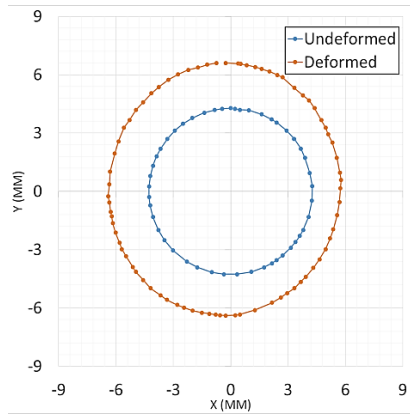
(c) $V=212.35$ m/s



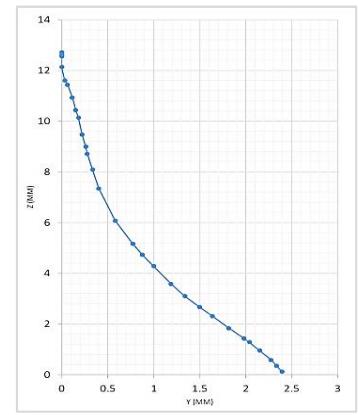
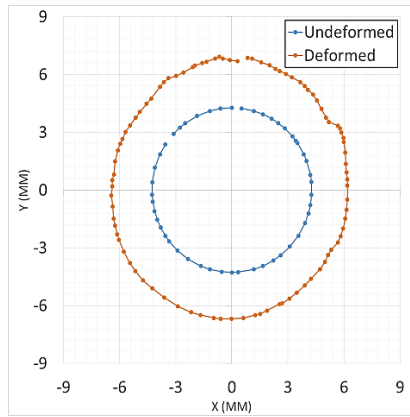
(d) $V=230.58$ m/s



(e) $V=257.45$ m/s



(f) $V=287.17$ m/s



(g) $V=302.13$ m/s

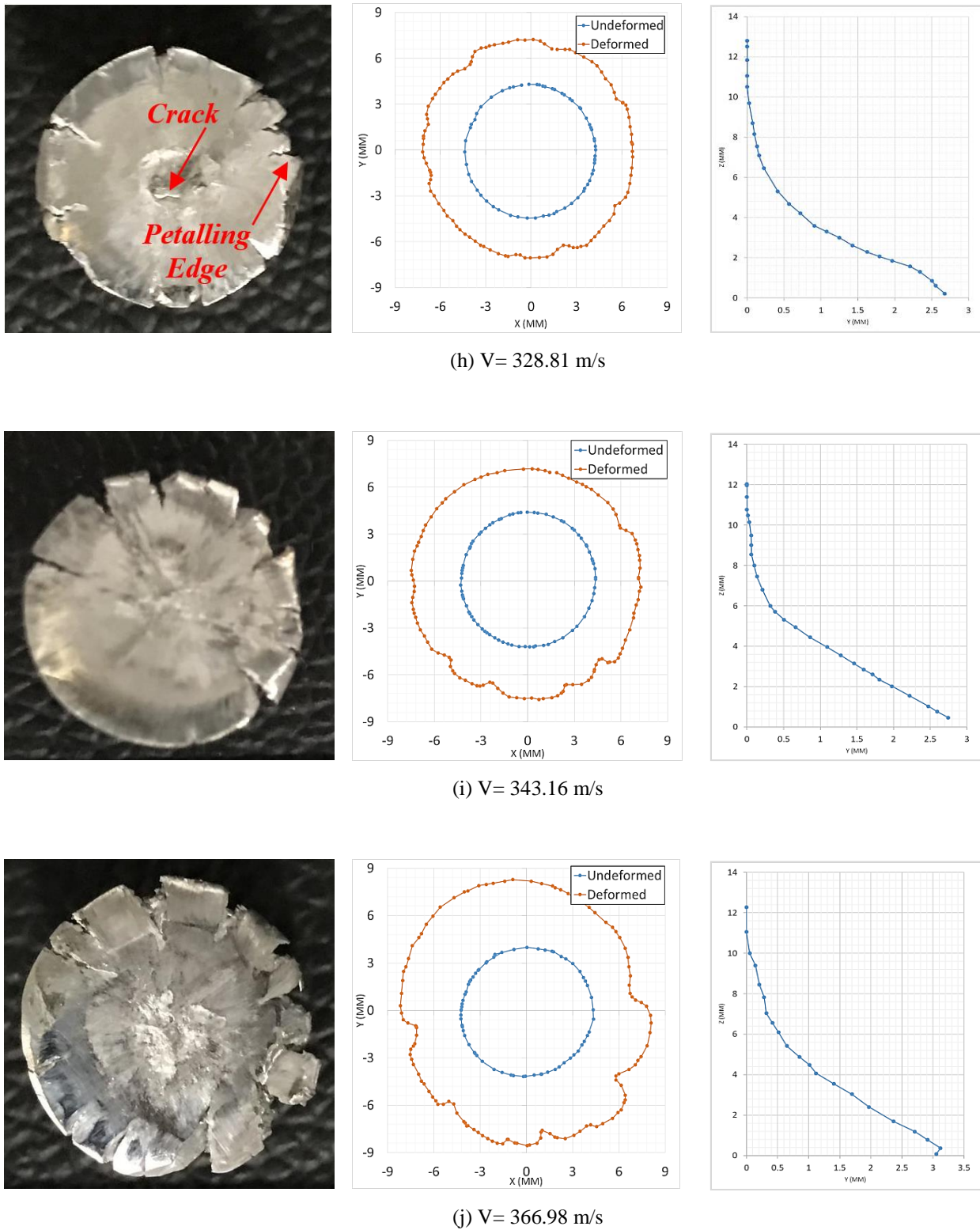


Figure 6. Deformed footprint and digitized data of recycled AA6061 at various impact velocities

Table 3 summarizes the experimental results of the impact test at different impact velocities. The deformed length and the distance of the major footprint profile are measured and recorded. Figure 7 depicts the sample of reference to define deformed length (L_d) and final length (L_f). Besides, the fracture mode, according to Figure 1, for each of the deformed specimen is clearly illustrated. From the results obtained, it can be noted that there are three types of fracture modes can be observed with the changes in impact velocity. The observations and behaviour for each of the fracture modes are presented below:

- i. **Mushrooming:** This fracture mode is driven by plastic deformation without visible cracks. It occurred during a projectile impacts a target at low velocity, and instantaneously, both elastic and plastic waves are generated at the

impact interface after impact. This type of fracture mode is observed at impact velocity ranging from 179 m/s to 212 m/s. There are no any visible cracks can be detected.

- ii. Tensile splitting: This fracture mode is observable on the specimen at an impact velocity of 230 m/s to 302 m/s. This fracture mode occurred due to the tensile hoop strain beyond the ductility of the material. Thus, referring to Figures 6(d) – (g), cracks are observed at the edge of the mushroomed end of the impact footprint. With the increases of impact velocity, the cracks are getting visible. At impact velocities 287 m/s and 302 m/s, the formation of cracks are quite distinct. Visible cracks can be observed at the side profile of the specimen (Figure 8).
- iii. Petalling: This fracture mode initiates by tensile splitting. Typical petalling shaped projectile after impact can be noticed at the specimen with an impact velocity of 328 m/s to the maximum impact velocity of 367 m/s (Figures 6(h) – (j)). Many visible cracks are observed, and sunflower-like petalling shaped is formed at the edge of the mushroomed end of the impact footprint.

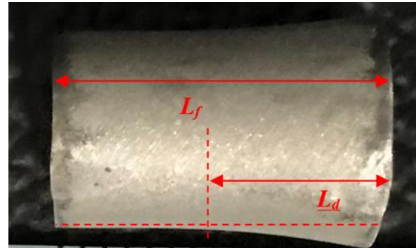


Figure 7. Reference to define L_d and L_f

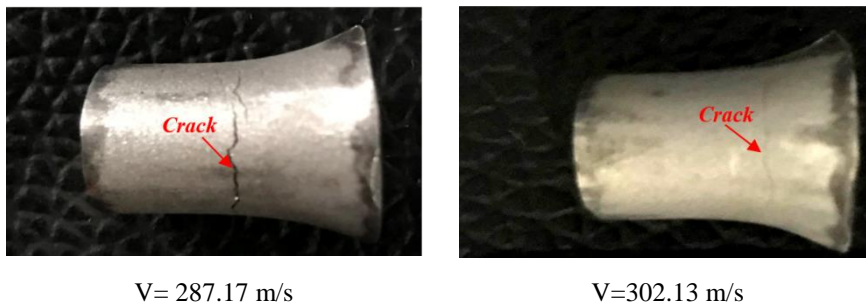


Figure 8. Sample of deformed side profile with visible crack

Table 3. Impact behaviour of recycled AA6061

| Impact Velocity, V (m/s) | Final Length, L_f (mm) | Deformed Length, L_d (mm) | Distance of Major Profile, D_d (mm) | Fracture Mode |
|--------------------------|--------------------------|-----------------------------|---------------------------------------|---|
| 179.01 | 13.84 | 7.50 | 10.09 | Mushrooming |
| 195.28 | 13.58 | 7.54 | 10.65 | Mushrooming |
| 212.35 | 13.48 | 7.77 | 10.24 | Mushrooming |
| 230.58 | 13.13 | 7.76 | 11.15 | Tensile Splitting + Cracks |
| 257.45 | 12.78 | 7.67 | 11.56 | Tensile Splitting + Cracks |
| 287.17 | 12.37 | 7.36 | 12.79 | Tensile Splitting + Cracks at the Edge and Side Profile |
| 302.13 | 12.15 | 7.29 | 13.25 | Tensile Splitting + Cracks at the Edge and Side Profile |
| 328.81 | 11.74 | 7.06 | 14.24 | Petalling + Cracks |
| 343.16 | 11.21 | 6.78 | 14.91 | Petalling + Cracks |
| 366.98 | 10.68 | 6.72 | 16.18 | Petalling + Cracks |

Metallurgical Investigation

The impact surface of some deformed specimens is observed under a scanning electron microscope (SEM) with a magnification scale of X500 to evaluate damage progression for each fracture mode. Besides, the microstructure of the specimen before the impact is also examined. Figure 9 and 10 illustrate the SEM micrographs of the deformed and undeformed specimens for each fracture modes, respectively.

Referring to Figure 9, micro-voids and dimples are observed in the undeformed specimen. This data concludes that damage characteristics are initiated and developed since the preparation of the specimen. The micro-voids and dimples are growing and coalesce further as material undergoing impact deformation. This phenomenon observable at the micro-scale level by the increment of quantity and size of the micro-voids and dimples, including the formation of micro-cracks. Fig. 10 illustrates the damage evolution. As can be seen, the amount of micro-voids, micro-cracks, and dimples are increasing as the impact velocity increases. Figure 10(b) and (c) show many cracks within the impact surface while less amount of voids are detected as the damage growth and coalescence at higher impact velocity to form splitting and petalling shaped edge. This indicates that the AA6061 still showing a strong strain rate dependency in their recycled form. The damage evolution causes severe localized plastic strain deformation, as shown by the footprint radial expansion and length reduction.

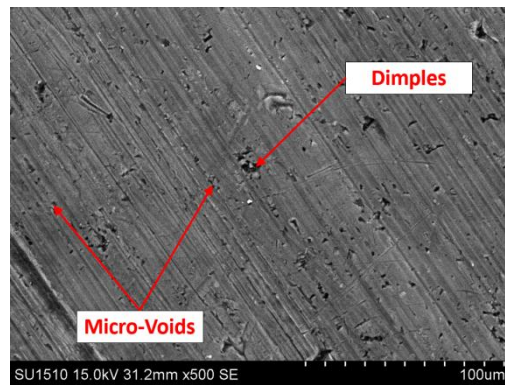
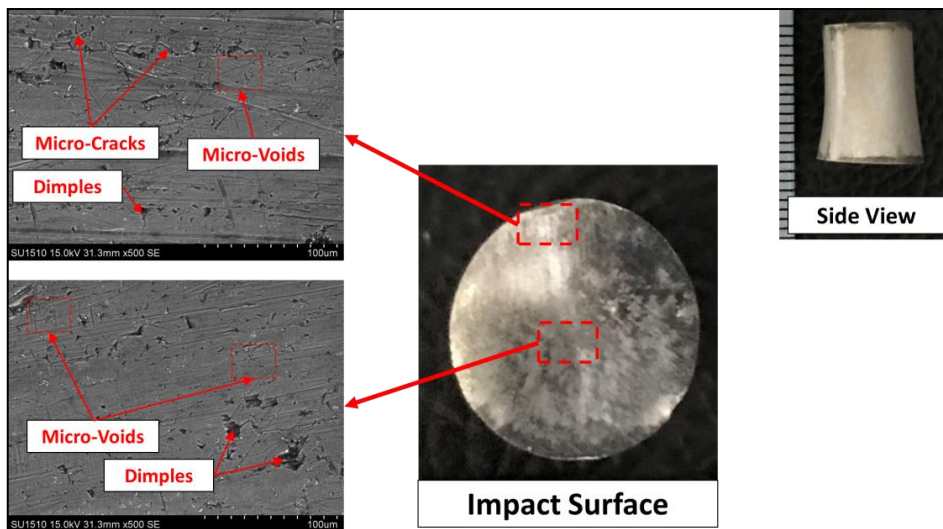
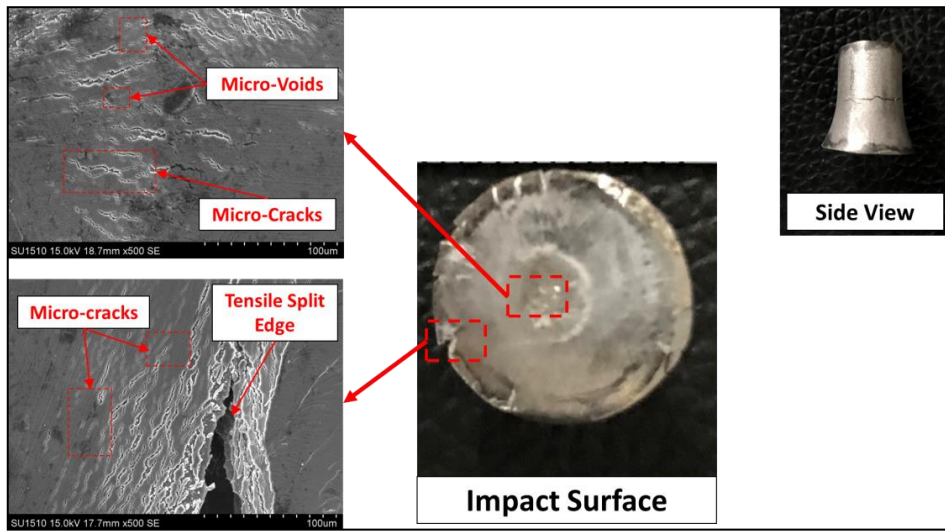


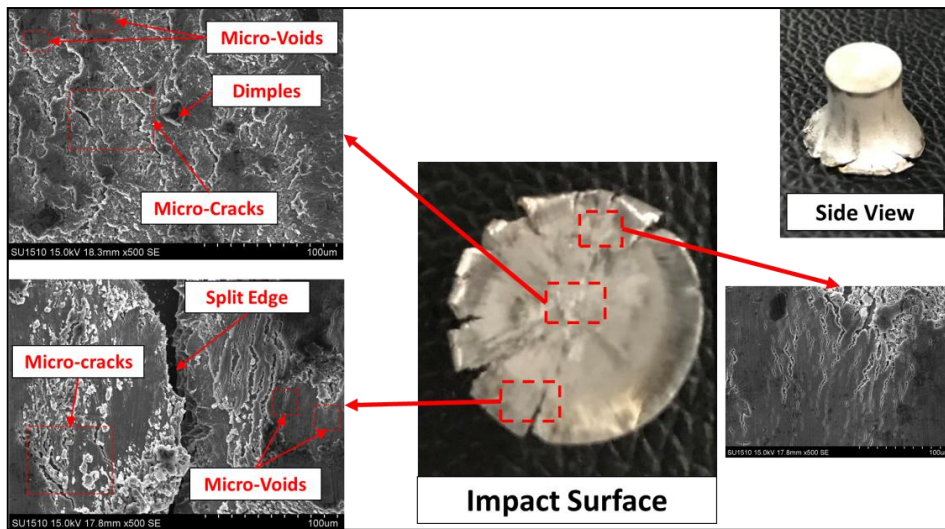
Figure 9. SEM micrographs of undeformed recycled AA6061 specimen



(a) $V = 195.28$ m/s



(b) $V = 287.17 \text{ m/s}$



(c) $V = 343.16 \text{ m/s}$

Figure 10. SEM micrographs at different point for specimen with different fracture mode: (a) Mushrooming, (b) Tensile Splitting, and (c) Petalling

Moreover, Figure 11 presents the SEM micrographs of the cross-section located 5mm above the impact surface of different fracture modes. Micro-cracks and micro-voids still can be observed around the surface due to the damage propagated from the impact surface towards the centre of the specimen. The damage progress due to localized plastic strain propagates into the material. Also, it can be observed that the length of the micro-cracks increases with increasing impact velocity.

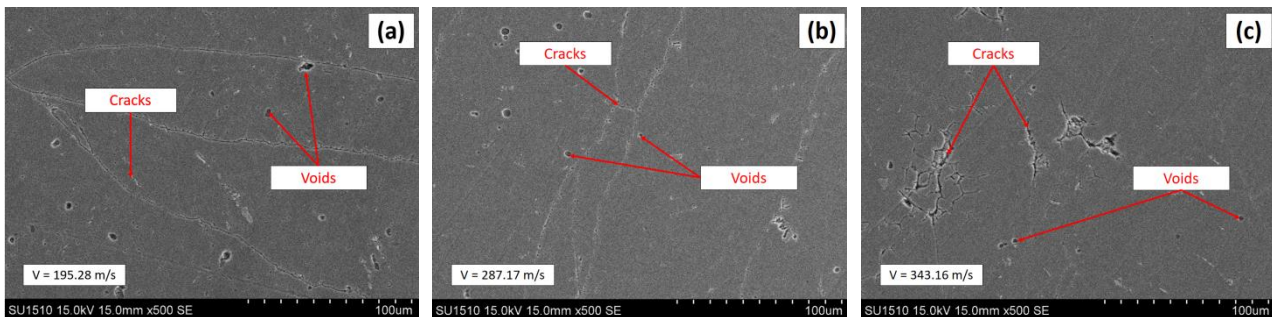


Figure 11. SEM micrograph of sectional area (5mm away from impact surface) at fracture mode of: (a) mushrooming, (b) Tensile Splitting, and (c) Petalling

CONCLUSION

This paper investigates the damage behaviour and its progression of recycled aluminium alloy AA6061 undergoing various impact velocity via Taylor cylinder impact testing. It is observed that such recycled AA6061 exhibited anisotropic behaviour with non-symmetric ellipse-shaped footprint of the deformed specimen. There are three different types of fracture modes can be observed for impact velocity range from 170 m/s to 370 m/s, named mushrooming, tensile splitting and petalling. The critical impact velocity of such recycled material is found to be lower than 212.35 m/s. Below this critical impact velocity, the material experiences localized plastic strain deformation to form mushrooming shape. Above this critical value, severe fracture modes of tensile splitting and petalling can be observed. In general, it can be concluded that such recycled material capable of showing ductile fracture mode that is influenced by nucleation, growth and coalescence of the micro-voids and dimples. This damage evolution is clearly presented by radial expansion of the footprint and reduction in length of the deformed specimen. Besides, the damage is also propagating from the impact surface towards the material. The propagation of the damage is getting severe with the increases in impact velocity. General speaking, the recycled AA6061 exhibits a strong strain rate dependency in which the damage evolution is increasing as the impact velocity increase cause severe localized plastic strain deformation. The result is promising for better application identification in advanced engineering applications. Further enhancement in terms of material process can be considered such as the inclusion of material reinforcement to provide fine-grained microstructure.

ACKNOWLEDGMENTS

Authors wish to convey sincere gratitude to Universiti Tun Hussein Onn Malaysia (UTHM) for providing the financial means during the preparation to complete this work under Geran Penyelidikan Pascasiswazah (GPPS), Vot U74 and UTHM Contract Research Grant, Vot H276. This research work is also supported by the Aerospace Manufacturing Research Center (AMRC), Faculty of Engineering, Universiti Putra Malaysia and the Sustainable Manufacturing and Recycling Technology, Advanced Manufacturing and Material Center (SMART AMMC), Faculty of Mechanical and Manufacturing Engineering, Universiti Tun Hussein Onn Malaysia.

REFERENCES

- [1] S. Kushnoore, V. Atgur, P. K. C. Kanigalpula, N. Kamitkar, and P. Shetty, "Experimental Investigation on Thermal Behavior of Fly Ash Reinforced Aluminium Alloy (Al6061) Hybrid Composite," *J. Mech. Eng. Sci.*, vol. 13, no. 3, pp. 5588–5603, 2019.
- [2] R. Bobbili, V. Madhu, and A. K. Gogia, "Tensile Behaviour of Aluminium 7017 Alloy at Various Temperatures and Strain Rates," *J. Mater. Res. Technol.*, vol. 5, no. 2, pp. 190–197, 2016.
- [3] N. K. Yusuf, M. A. Lajis, M. I. Daud, and M. Z. Noh, "Effect of Operating Temperature on Direct Recycling Aluminium Chips (AA6061) in Hot Press Forging Process," *Appl. Mech. Mater.*, vol. 315, pp. 728–732, 2013.
- [4] I. Sabry and A. M. El-Kassas, "An Appraisal of Characteristic Mechanical Properties and Microstructure of Friction Stir Welding for Aluminium 6061 Alloy - Silicon Carbide (SiCp) Metal Matrix Composite," *Journal Mech. Eng. Sci.*, vol. 13, no. 4, pp. 5804–5817, 2019.
- [5] M. W. A. Rashid, F. F. Yacob, M. A. Lajis, M. A. A. M. Abid, and E. M. T. Ito, "A Review: The Potential of Powder Metallurgy in Recycling Aluminum Chips (Al 6061 & Al 7075)," in *Conference: 24th Design Engineering Systems Division JSME Conference Japan Society of Mechanical Engineers*, 2014, pp. 14–27.
- [6] M. S. Shahrom, A. R. Yusoff, and M. A. Lajis, "Taguchi Method Approach for Recycling Chip Waste from Machining Aluminum (AA6061) Using Hot Press Forging Process," *Adv. Mater. Res.*, vol. 845, pp. 637–641, 2013.
- [7] B. L. Chan and M. A. Lajis, "Direct Recycling of Aluminium 6061 Chip Through Cold Compression," *Int. J. Eng. Technol.*, vol. 15, no. 04, pp. 4–8, 2015.
- [8] Y. Kume, T. Takahashi, M. Kobashi, and N. Kanetake, "Solid State Recycling of Die-cast Aluminum Alloy Chip Wastes by Compressive Torsion Processing," *Keikin-zoku/Journal Japan Inst. Light Met.*, vol. 59, no. 7, pp. 354–358, 2009.
- [9] S.-H. Hong, D.-W. Lee, and B.-K. Kim, "Manufacturing of Aluminum Flake Powder from Foil Scrap by Dry Ball Milling Process," *J. Mater. Process. Technol.*, vol. 100, pp. 105–109, 2000.
- [10] S. Kumar, F. Mathieux, G. Onwubolu, and V. Chandra, "A Novel Powder Metallurgy-based Method for the Recycling of Aluminum Adapted to a Small Island Developing State in the Pacific," *Int. J. Environ. Conscious Des.*, vol. 13, no. 3.4, pp. 1–22, 2007.
- [11] M. Rahimian, N. Ehsani, N. Parvin, and H. reza Baharvandi, "The Effect of Particle Size, Sintering Temperature and Sintering Time on the Properties of Al-Al₂O₃ Composites, Made by Powder Metallurgy," *J. Mater. Process. Technol.*, vol. 209, no. 14, pp. 5387–5393, 2009.
- [12] M. Rahimian, N. Parvin, and N. Ehsani, "The Effect of Production Parameters on Microstructure and Wear Resistance of Powder Metallurgy Al–Al₂O₃ Composite," *Mater. Des.*, vol. 32, no. 2, pp. 1031–1038, 2011.
- [13] A. Ahmad, M. A. Lajis, N. K. Yusuf, S. Shamsudin, and Z. W. Zhong, "Parametric Optimisation of Heat Treated Recycling Aluminium (AA6061) by Response Surface Methodology," in *AIP Conference Proceedings*, 2017, vol. 1885, no. 1, pp. 1–7.
- [14] S. N. A. Rahim, M. A. Lajis, and S. Ariffin, "Effect of Extrusion Speed and Temperature on Hot Extrusion Process of 6061 Aluminum Alloy Chip," *ARPJ. Eng. Appl. Sci.*, vol. 11, no. 4, pp. 2272–2277, 2016.

- [15] M. Haase and A. E. Tekkaya, "Recycling of Aluminum Chips by Hot Extrusion with Subsequent Cold Extrusion," in *Procedia Engineering*, 2014, vol. 81, pp. 652–657.
- [16] A. E. Tekkaya, M. Schikorra, D. Becker, D. Biermann, N. Hammer, and K. Pantke, "Hot Profile Extrusion of AA-6060 Aluminum Chips," *J. Mater. Process. Technol.*, vol. 209, no. 7, pp. 3343–3350, 2009.
- [17] S. S. Khamis, M. A. Lajis, and R. A. O. Albert, "A Sustainable Direct Recycling of Aluminum Chip (AA6061) in Hot Press Forging Employing Response Surface Methodology," *Procedia CIRP*, vol. 26, pp. 477–481, 2015.
- [18] N. K. Yusuf, M. A. Lajis, and A. Ahmad, "Hot Press as a Sustainable Direct Recycling Technique of Aluminium : Mechanical Properties and Surface Integrity," *Materials (Basel)*, vol. 10, no. 8, p. 902, 2017.
- [19] A. Ahmad, M. A. Lajis, and N. K. Yusuf, "On the Role of Processing Parameters in Producing Recycled Aluminum AA6061 Based Metal Matrix," *Materials (Basel)*, vol. 10, no. 1098, pp. 1–15, 2017.
- [20] M. A. Lajis, S. S. Khamis, and N. K. Yusuf, "Optimization of Hot Press Forging Parameters in Direct Recycling of Aluminium Chip (AA 6061)," *Key Eng. Mater.*, vol. 622–623, pp. 223–230, 2014.
- [21] M. K. M. Nor, N. Ma'at, and C. S. Ho, "An Anisotropic Elastoplastic Constitutive Formulation Generalised for Orthotropic Materials," *Contin. Mech. Thermodyn.*, vol. 30, no. 7, pp. 1–36, 2018.
- [22] M. K. M. Nor, "Modeling of Constitutive Model to Predict the Deformation Behaviour of Commercial Aluminum Alloy AA7010 Subjected to High Velocity Impacts," *ARPJ J. Eng. Appl. Sci.*, vol. 11, no. 4, pp. 2349–2353, 2016.
- [23] A. L. Noradila, Z. Sajuri, J. Syarif, Y. Miyashita, and Y. Mutoh, "Effect of Strain Rates on Tensile and Work Hardening Properties for Al-Zn Magnesium Alloys," *Int. J. Mater. Eng. Innov.*, vol. 5, no. 1, pp. 28–37, 2014.
- [24] M. K. M. Nor, R. Vignjevic, and J. Campbell, "Modelling of Shockwave Propagation in Orthotropic Materials," *Appl. Mech. Mater.*, vol. 315, pp. 557–561, 2013.
- [25] S. Castagne, A. Habraken, and S. Cescotto, "Application of a Damage Model to an Aluminium Alloy," *J. Damage Mech.*, vol. 12, no. 1, pp. 5–30, 2003.
- [26] B. Wan, W. Chen, T. Lu, F. Liu, Z. Jiang, and M. Mao, "Review of Solid State Recycling of Aluminum Chips," *Resour. Conserv. Recycl.*, vol. 125, pp. 37–47, 2017.
- [27] A. Balasundaram, A. M. Gokhale, S. Graham, and M. F. Horstemeyer, "Three-dimensional Particle Cracking Damage Development in an Al-Mg-base Wrought Alloy," *Mater. Sci. Eng. A*, vol. 355, no. 1–2, pp. 368–383, 2003.
- [28] N. Ma'at, K. A. Kamarudin, and A. E. Ismail, "Implementation of Finite Strain-Based Constitutive Formulation in LLLNL-DYNA3D to Predict Shockwave Propagation in Commercial Aluminum Alloys AA7010," *Int. Eng. Res. Innov. Symp.*, vol. 160, no. 1, p. 012023, 2016.
- [29] M. K. M. Nor, "Modelling Inelastic Behaviour of Orthotropic Metals in a Unique Alignment of Deviatoric Plane within the Stress Space," *Int. J. Non-Linear Mech.*, vol. 87, pp. 43–57, 2016.
- [30] V. Panov, "Modelling of Behaviour of Metals at High Strain Rates," Ph.D. Thesis, Cranfield University, 2006.
- [31] S. Abdullah, M. F. Abdullah, and W. N. M. Jamil, "Ballistic Performance of the Steel-Aluminium Metal Laminate Panel for Armoured Vehicle," *J. Mech. Eng. Sci.*, vol. 14, no. 1, pp. 6452–6460, 2020.
- [32] G. Taylor, "The Use of Flat-Ended Projectiles for Determining Dynamic Yield Stress. II. Tests on Various Metallic Materials," *Proc. R. Soc. A Math. Phys. Eng. Sci.*, vol. 194, no. 1038, pp. 300–322, 1948.
- [33] P. J. Maudlin, J. F. Bingert, J. W. House, and S. R. Chen, "On the Modeling of the Taylor Cylinder Impact Test for Orthotropic Textured Materials: Experiments and Simulations," *Int. J. Plast.*, vol. 15, no. 2, pp. 139–166, 1999.
- [34] K. G. Rakvåg, T. Børvik, and O. S. Hopperstad, "A Numerical Study on the Deformation and Fracture Modes of Steel Projectiles during Taylor Bar Impact Tests," *Int. J. Solids Struct.*, vol. 51, no. 3–4, pp. 808–821, 2014.
- [35] K. G. Rakvåg, T. Børvik, I. Westermann, and O. S. Hopperstad, "An Experimental Study on the Deformation and Fracture Modes of Steel Projectiles during Impact," *Mater. Des.*, vol. 51, pp. 242–256, 2013.
- [36] C. A. Acosta, C. Hernandez, and A. Maranon, "Validation of Material Constitutive Parameters for the AISI 1010 Steel from Taylor Impact Tests," *Mater. Des.*, vol. 110, pp. 324–331, 2016.
- [37] Z. Cao, "Investigation of Taylor Impact Test of Isotropic and Anisotropic Material Through Geometrical Characteristics of Specimens," Degree of Master Thesis, University of Alabama, 2010.
- [38] C. S. Ho et al., "Characterization of Anisotropic Damage Behaviour of Recycled Aluminium Alloys AA6061 Undergoing High Velocity Impact," *Int. J. Integr. Eng.*, vol. 11, no. 1, pp. 247–256, 2019.